Available online at www.sciencedirect.com
SciVerse ScienceDirect
Energy Procedia 37 (2013) 5055 – 5062
Energy Procedia

GHGT-11

Core and Pore Scale Characterization of Liujiagou Outcrop Sandstone, Ordos basin, China for CO_2 Aquifer Storage

WANG Yan[a], Dustin Crandall[b,c], Kathy Bruner[b,c,d], WEI Ning[a],
Magdalena Gill[b,c], LI Xiaochun[a*], Grant Bromhal[b]

[a] *State Key Laboratory for Geo-mechanics and Geo-technical Engineering, Institute of Rock and Soil Mechanics, Chinese Academy of Sciences, Wuhan 430071, China*
[b] *United States Department of Energy, National Energy Technology Laboratory, Morgantown WV 26507, United States*
[c] *URS Corporation, Morgantown WV 26507, United States*
[d] *West Virginia University, Department of Geology, Morgantown, WV 26506, United States*

Abstract

This paper describes various laboratory studies that have been performed on Liujiagou sandstone samples from the Ordos basin. The sample characterization includes multi-scale X-ray computed tomography (CT) scanning, and thin section petrographic analysis. Core scale and pore scale characterizations of the Liujiagou formation sandstone were obtained. Injection of liquid CO_2 into a brine saturated Liujiagou sandstone core was performed until a steady state condition was observed within a CT scanner. The CO_2 filled some of the pore space, moving quickly through the laminae and/or bedding planes of core that were open. Pore/grain scale analysis via thin section petrography classified the Liujiagou sandstone as an arkosic arenite with a quartz/feldspar/rock fragment ratio of 51/32/17 and a mean grain size of 0.35 mm. Primary pores are generally clean and account for 1% of the overall porosity, which was measured as 6% within the thin section analyzed. Understanding how these pore and core scale characteristics of Liujiagou sandstone affect fluid migration through this important Chinese resource will be instrumental in the planning and operation of future CCUS projects.

Selection and/or peer-review under responsibility of GHGT

Keywords: Ordos basin, Liujiagou, characterization, saline aquifer, computed tomography, CO_2 flooding, thin section petrography

The Ordos Basin, located in northwest China, is the second largest basin in China. It holds abundant natural fossil energy resources[1]. Many large stationary sources of CO_2 are in the area, and vast amounts of subsurface storage volume may be found within deep saline aquifers in the 360,000 km^2 basin. From

* Corresponding author. Tel.: +86-27-87197135; fax: +86-27-87198967.
E-mail address: xcli@whrsm.ac.cn; ywang@whrsm.ac.cn.

1876-6102
Selection and/or peer-review under responsibility of GHGT
doi:10.1016/j.egypro.2013.06.419

the preliminary source-sink matching results [2], the basin is ideally located for large-scale deployment of CO_2 capture, utilization, and storage technologies (CCUS). The Early Triassic Liujiagou Formation is a deep saline sandstone aquifer that is being evaluated for its potential for large scale CO_2 sequestration. Core samples from outcrops are being characterized using multi-scale X-ray CT scans, thin section petrography, and other measurements to determine the formation's suitability for carbon storage. In this paper, "Sample L", indicates the sample came from the Liujiagou Formation.

1. Multi-scale X-ray CT scans

Three scanners were used to characterize the structure of Sample L. Dry scans from a medical CT scanner (Univeral Systems HD 350-E) revealed that the samples have very distinct bedding planes comprised of coarser sand grains. Industrial CT scans with a North Star Imaging scanner of Sample L revealed with greater clarity that the laminations in the core were regularly spaced, consisted of alternating high/low bulk densities, and were oriented at a dip angle of approximately 30°. With a micro-CT scanner (Xradia MicroXCT-400) 2μm and 11μm resolution scans of sub-cores from Sample L showed in-filling of calcite in some regions and a near complete lack of calcite in other zones (Fig 1).

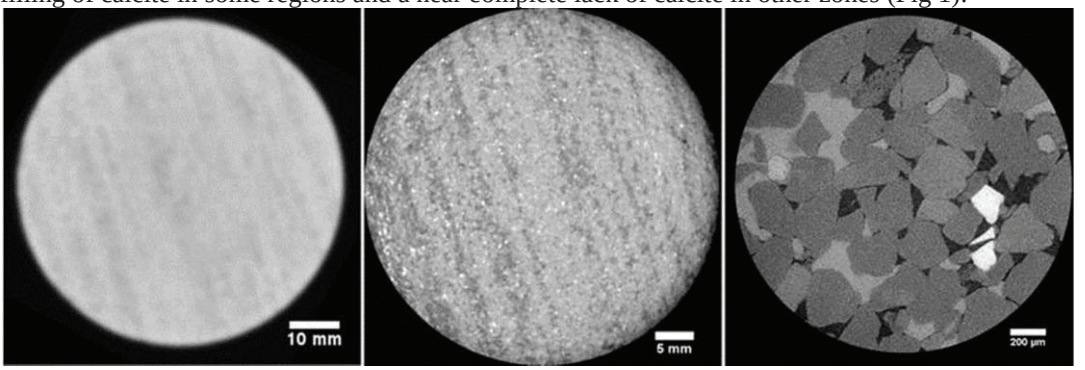

Fig. 1. 2D cross-section through sample L from the medical, industrial & micro-CT scanners. In this image darker zones within the sandstone are lower density regions, i.e. higher porosity; lighter areas are relatively higher density, i.e. lower porosity.

1.1. CO_2 flooding of Sample L in the medical CT scanner.

A flow through test of CO_2 displacing brine within Sample L showed that the CO_2 preferentially flowed through the less dense planes.

- Initial core properties:
  Weight = 754.6 g, Diameter = 2 inch (5.08 cm), Length = 6.017 in (15.283 cm),
  Saturated with distilled water under vacuum for 48 hours+
  Wet weight = 776.5 g, Calculated porosity = 0.0707.
- Description of Core Flood:

At the condition of pore pressure = 2200 psi, Confining pressure = 2450 psi, Room temperature= 72 °F, core initially saturated with 5 wt% KI brine. Injection of liquid CO_2 at a constant rate of 0.2 ml/min was then performed until a steady state condition was observed.

Pressure was maintained within the system by injecting and withdrawing from the system with 2 ISCO pumps. Axial CT scans during the flooding experiment were taken with a resolution of 0.25 mm by 0.25

mm by 5 mm. The coarse axial resolution enabled rapid scanning of the entire core and subsequent capture of the CO_2 front motion.

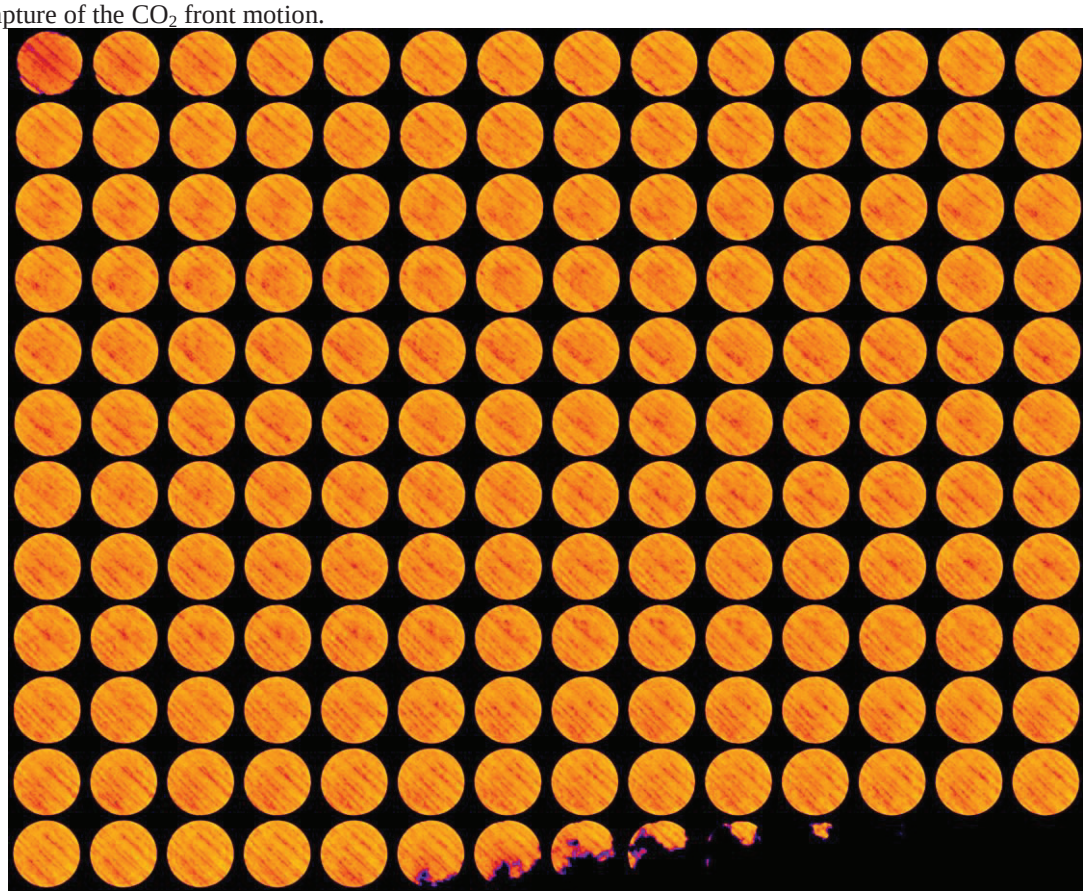

Fig. 2. Dry CT scan of Sample L prior to flooding with 1mm thick slices. In this false-color image darker zones within the sandstone are lower density regions, i.e. higher porosity.

Analysis:

The initial CO_2 front moved directly through high-porosity/high-permeability laminae/bedding planes (Figure 4). Due to the unique coring of this sample, with the bedding planes angled, this front propagation was easily determined to occur within a higher-porosity bedding plane that spanned the length of the sample. Because of this flow within the relatively small preferential flow path, the total amount of pore-volume (PV) filled by the time the CO_2 reached the exit manifold was quite small (0.16 ml CO_2 injected, or 7% PV filled, Table 1).

Table 1. Time of 1st scan in each series and approximate Pore Volume (PV) injected at that time

1:59 PM	2:07 PM	2:14 PM	2:22 PM	2:29 PM	2:45 PM	3:10 PM	3:48 PM
0 PV	0.07 PV	0.14 PV	0.20 PV	0.26 PV	0.40 PV	0.63 PV	0.98 PV

After the initial front breakthrough occurred the CO_2 began filling in other higher porosity bedding planes, as shown by lower Computed Tomography Number (CTN) values along the length of the core at angles approximately equal to the original breakthrough CO_2 plume (Figure 3). Perhaps most interestingly, over the course of the experiment this continual filling of bedding planes with CO_2 resulted in a nearly uniform decrease in the CTN across the length of the sample (Figure 3, plot on right). The differences in absolute CTN can be attributed to sub-core scale heterogeneities (e.g. Figure 2; the ratio of high and low porosity regions within each 1mm thick slice are not equal). But, the nearly uniform decrease in CTN between subsequent experiments shown in Figure 2 indicate that the CO_2 was moving quickly through the entire length of the core and reducing the measured bulk density of the sample over each region of interest nearly uniformly for over an hour. The CT scans at 3:48 PM and 3:10 PM resulted in nearly identical CTN values, suggesting that the CO_2 distribution had reached a steady state within the sample after approximately an hour of injection at 0.2 ml/min.

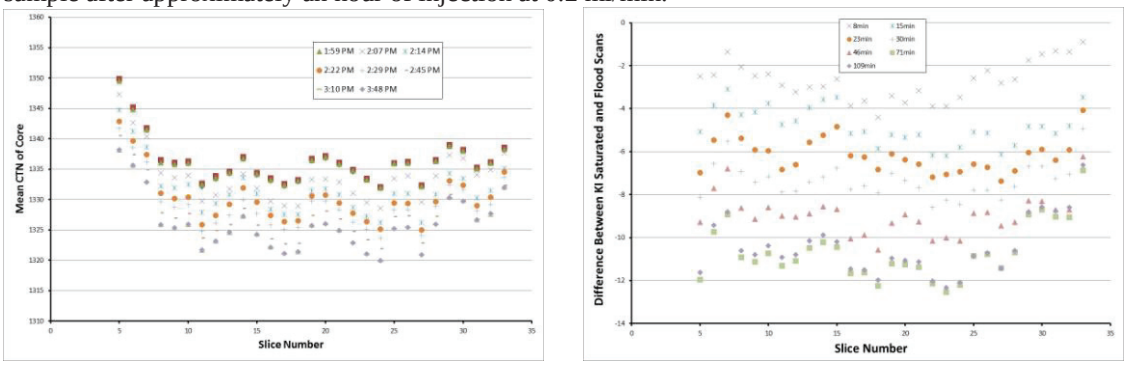

Fig. 3. Left: Mean CT number (CTN) of each 5mm thick scan. Lower numbers indicate a greater infiltration of CO_2. Time stamps in legend refer to the time of the first CT scan in each series: total time to scan core was approximately 8 minutes. Right: Difference between the CTN of the core saturated with brine and the CO_2/brine mixture within the core. Note the fairly consistent decrease in CTN across the length of the core for each time step.

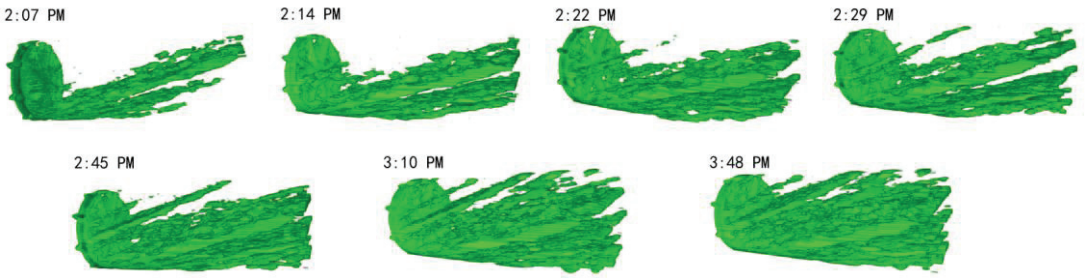

Fig.4. 3D reconstruction of CO_2 within the sandstone over the course of the flood. Gas inlet side, with the fluid distribution channels, shown on the left and the CO_2 is shown in green. The 7 images correspond to scans taken at 2:07 PM, 2:14 PM, 2:22 PM, 2:29 PM, 2:45 PM, 3:10 PM & 3:48 PM.

1.2. Micro CT Scans

Six micro CT scans were performed on sandstone cores from the Liujiagou Formation outcrop. Three of these scans imaged the entire 0.25 inch diameter sub-cores, with a resolution of 11 um. The remaining three were micro CT scans, performed on sub-sections of the small sub-cores, with a much higher resolution of 2 um. Parallel studies of sandstone thin sections allowed for the identification of several discrete phases within the rock: open pore space, calcite cement, framework grains, and heavy mineral grains. The different specific gravity of each constituent allowed for their subsequent separation in the CT scan images. Constituents were identified and analyzed using ImageJ [3] image processing software, and a calculation was performed on each image to assess the relative amounts of each constituent.

Each of the four constituents (pore space, framework grains, calcite cement, and heavy minerals) were defined by the selection of two bounding gray scale thresholds with recorded values. The results of this high and low estimate were then averaged to obtain a final value. The results were summed along the entire length of core, resulting in a total volume and percentage estimate for each constituent within the core. The four constituent fractions are then summed to ensure consistent analysis; a result approaching 100% of the total volume of the sample confirms reliability of the analysis.

Table 2. Sample L Core Makeup from Micro-CT Scans

	Scan Resolution	Porosity	Calcite	Framework Grains	Heavy Minerals	Total
Scan 1	11 μm	9.32%	15.57%	73.11%	2.09%	100.09%
Scan 2	11 μm	7.81%	17.30%	73.75%	1.14%	100.0%
Scan 3	11 μm	11.73%	8.11%	76.70%	3.52%	100.05%
Scan 4	2 μm	8.17%	27.01%	63.41%	1.8%	100.4%
Scan 5	2 μm	6.83%	22.74%	68.59%	0.16%	98.32%
Scan 6	2 μm	9.41%	18.14%	67.08%	1.71%	96.33%

A further analysis was performed on Scan 2, to gain an enhanced understanding of the interactions between the four phases. The varying percentages of constituents can be linked to the bedding contained in the sample. The general trends are as follows:

a. Calcite cement and porosity show a strong inverse relationship, as a lack of cement is directly linked to higher porosity values

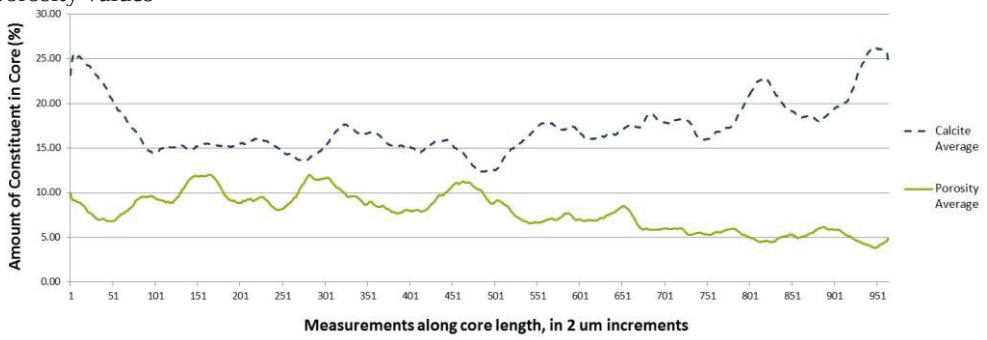

Fig. 5.Calcite Cement vs. porosity in scan 2

b. Porosity shows a possible weak inverse relationship to framework grains, suggesting that some framework grain dissolution may be enhancing porosity. This finding is consistent with moldic porosity, formed after dissolution of rock fragments and feldspars, as seen in certain thin section photos.

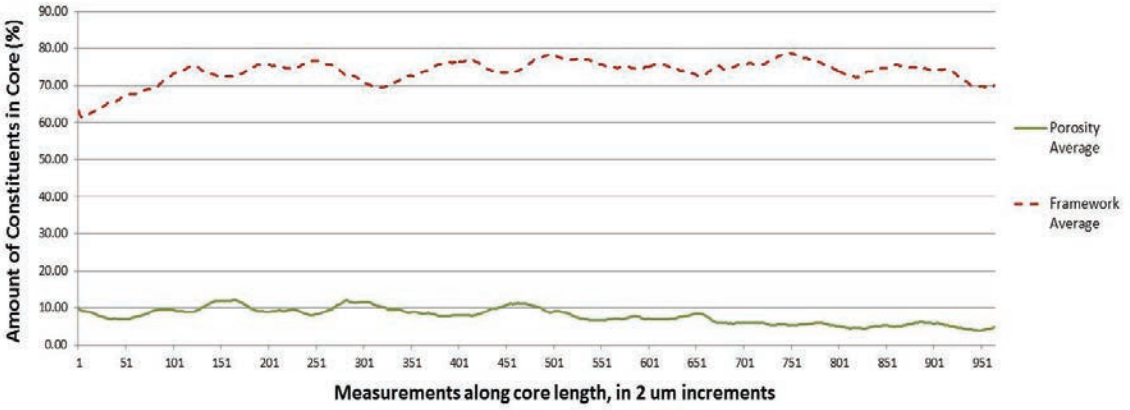

Fig. 6. Porosity vs. framework grains in scan 2

c. Calcite cement and framework grains also display an inverse relationship. A larger proportion of framework grains would directly preclude the formation of large amounts of calcite cement, by reducing the available intragranular space.

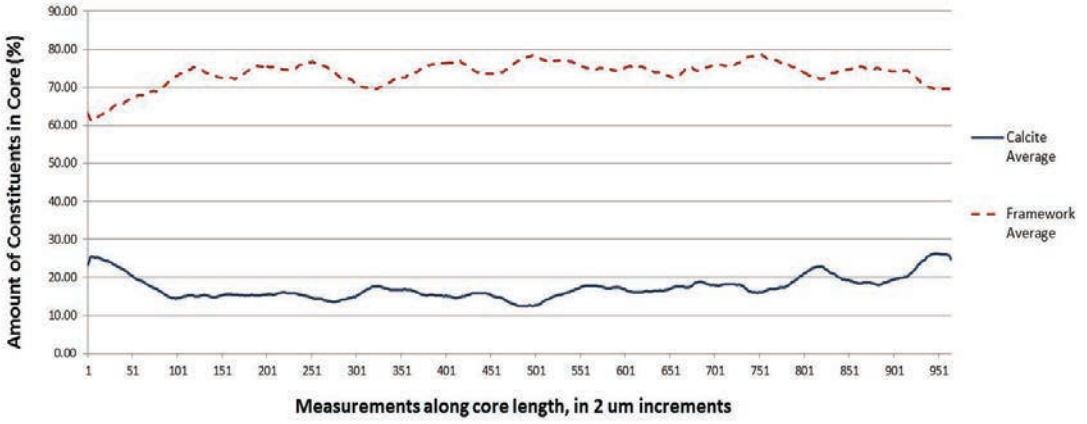

Fig. 7. Calcite Cement vs. framework grains in scan 2

d. Porosity does not display any strong relationship to the amount of framework grains.
e. Heavy minerals are concentrated in bands, most likely along laminate/bedding planes, as is apparent in their uneven distribution. Four distinct concentrations of heavy minerals can be identified in scan 2, three of which can be linked to bands with increased porosity, i.e. bedding planes. The fourth peak in heavy mineral concentration is housed within a low porosity zone.

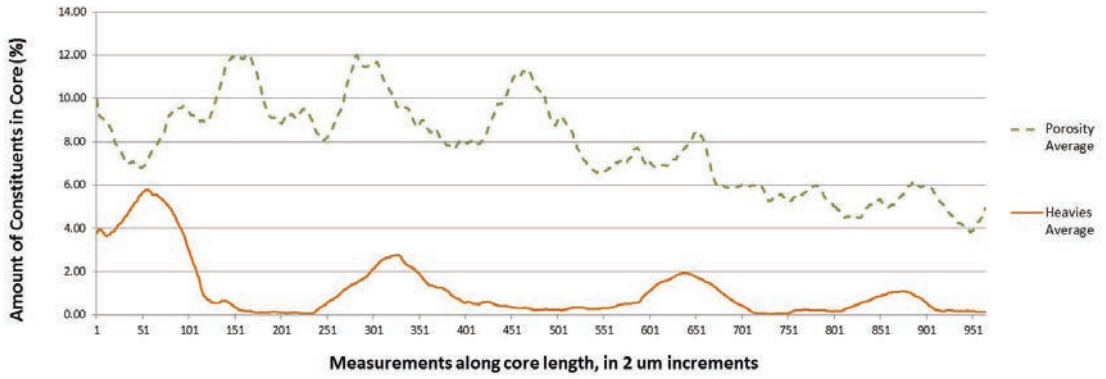

Fig. 8. Calcite Cement vs. porosity in scan 2

2. Thin Section Petrography

2.1. Detrital Constituents And Sedimentary Structures

The rock in thin section Sample L is classified as an arkosic arenite with a Q/F/RF = 51/32/17. Quartz is medium-grained, well-sorted, and sub-angular to sub-rounded. Mean grain size is 0.35 mm. Potassium feldspars are abundant, comprising 16 percent of the sample. They are rarely altered and show no evidence of partial dissolution. Plagioclase and perthite feldspars account for 12 percent of the rock; they are commonly altered, but rarely dissolved. Volcanic and metamorphic rock fragments comprise 6 percent of the sample. Included in this group are polycrystalline quartz, grains composed of fine quartz and feldspar within amicro/cryptocrystalline matrix, and sericite-rich framework grains. Other grains present in small amounts are sedimentary rock fragments, chert, chalcedony, biotite, garnet, zircon, epidote, and opaques. Chert is typically dirty in appearance as a result of vacuoles and inclusions such as chlorite and zircon. Clay coatings on grains are present but not common.

The sample exhibits low angle lamination, which is characterized by an increase in fine grained rock fragments, micas, and porosity.

2.2. Cement, Authigenic Minerals, And Matrix

Authigenic quartz is present in trace amounts. It typically occurs as syntaxial, incipient overgrowths, and small prismatic overgrowths nucleating on framework quartz grains and extending into open pores. Some of the overgrowths are large and euhedral. Dust rims are well-developed.

Calcite constitutes 16 percent of the sample and is the primary cementing agent. It occurs as large poikilotopic cement crystals. In rare cases, calcite that has replaced a pre-existing grain preserves a ghost of the grain in the cement.

Ductile deformation of framework grains forming psuedomatrix is rare.

2.3. Porosity

Porosity, as calculated by thin section analysis, accounts for 6 percent of the rock volume. Primary pores are generally clean and account for 1 percent porosity. Secondary pores enhance the primary pore

space. Porosity has preferentially developed along the lamination. Secondary pores are formed by the partial to total dissolution of rock fragments with lesser amounts of feldspar dissolution involved in the process.

Adjacent grains may be coated with fine mica or sericite/clay from the remnant material of the pre-existing grain.

The increase in porosity along the lamina in the sample is the result of several processes: the increase in unstable framework grains that can be dissolved, increased fluid flow as the secondary porosity develops, and a decrease in the amount of calcite cement as fluids transport available calcium carbonate through the laminae, thus considerably reducing the precipitation of the calcite cement.

3. Discussion

Core scale analysis indicated a slightly higher porosity of 7.1%, which is most likely due to the different scales and dimensions of analysis, and possibly core heterogeneity. Porosity developed preferentially along laminations within the core; secondary pores formed by the partial to total dissolution of rock fragments with lesser amounts of feldspar dissolution in the process. Understanding how these pore and core scale characteristics of Liujiagou sandstone affect fluid migration through this important Chinese resource will be instrumental in the planning and operation of future CCUS projects.

Additional work has been performed (XRD, SEM, porosity and permeability measurements)to further characterize these cores. Results will be analyzed to help improve our understanding of the CO_2 storage capability of the Liujiagou Formation.

Acknowledgements

The authors would like to acknowledge the financial support provided by Projects of International Cooperation from Ministry of Science and Technology of China, Joint Research on Low Emission Technologies for Integrated Gasification Combined Cycle (Grant number: 2010DFB70560) and Joint Research on Key Technologies of Oxy-fuel Combustion based CO2 Capture and Storage (Grant number: 2012DFB60100).

This technical effort was performed in support of the National Energy Technology Laboratory's ongoing research in CO_2 Storage under the RES contract DE-FE0004000.

References

[1] Li G , Lu M. *Atlas of oil and gas basins in China*. Petroleum Industry Publishing House, Beijing, China; 1988.

[2] Li X, Wei N, et al.. CO_2 point emission and geological storage capacity in China. *Energy Procedia* 2009;1:2793-2800.

[3] Rasband, W.S., ImageJ, U. S. National Institutes of Health, Bethesda, Maryland, USA, http://imagej.nih.gov/ij/, 1997-2012.